THE JOURNAL OF BIOLOGICAL CHEMISTRY VOL. 285, NO. 30, pp. 23342–23350, July 23, 2010

Novel Functions of *Stomatal Cytokinesis-Defective 1* (*SCD1*) in Innate Immune Responses against Bacteria*[S]

Received for publication, December 7, 2009, and in revised form, April 29, 2010 Published, JBC Papers in Press, May 14, 2010, DOI 10.1074/jbc.M109.090787

David A. Korasick[‡], Colleen McMichael[§], Katie A. Walker[‡1], Jeffrey C. Anderson[‡], Sebastian Y. Bednarek[§], and Antje Heese[‡2]

From the [‡]Interdisciplinary Plant Group (IPG), Division of Biochemistry, University of Missouri-Columbia, Columbia, Missouri 65211 and the [§]Department of Biochemistry, University of Wisconsin-Madison, Madison, Wisconsin 53706

Eukaryotes employ complex immune mechanisms for protection against microbial pathogens. Here, we identified *SCD1* (*Stomatal Cytokinesis-Defective 1*), previously implicated in growth and development through its role in cytokinesis and polarized cell expansion (Falbel, T. G., Koch, L. M., Nadeau, J. A., Segui-Simarro, J. M., Sack, F. D., and Bednarek, S. Y. (2003) *Development* 130, 4011–4024) as a novel component of innate immunity. In Arabidopsis, *SCD1* is a unique gene encoding for the only protein containing a complete DENN (Differentially Expressed in Normal and Neoplastic cells) domain. The DENN domain is a largely uncharacterized tripartite protein motif conserved among eukaryotic proteins. We show that conditional *scd1-1* plants containing a point mutation in a conserved DENN residue affected a subset of signaling responses to some bacterial pathogen-associated molecular patterns (PAMPs). Consistent with increased transcript accumulation of *Pathogen-related* (*PR*) genes, *scd1-1* plants were more resistant to *Pseudomonas syringae* pathovar *tomato* (*Pst*) DC3000 infection implicating SCD1 as a negative regulator of basal resistance against bacteria. *scd1-1* plants were different from known mutants exhibiting *constitutive expressor of PR* (*cpr*)-like phenotypes, in that growth impairment of *scd1-1* plants was genetically independent of constitutive immune response activation. For *scd1-1*, shift to elevated temperature or introduction of a mutant allele in *Salicylic acid Induction-Deficient 2* (*SID2*) suppressed constitutive defense response activation. *sid2-2* also repressed the resistance phenotype of *scd1-1*. Temperature shift and *sid2-2*, however, did not rescue conditional growth and sterility defects of *scd1-1*. These results implicate *SCD1* in multiple cellular pathways, possibly by affecting different proteins. Overall, our studies identified a novel role for eukaryotic DENN proteins in immunity against bacteria.

In eukaryotes, the first line of immunity against invading microbial pathogens occurs when host cell surface receptors sense potential microbial pathogens by recognizing pathogen-associated molecular patterns (PAMPs).[3] PAMP perception activates signaling pathways contributing to restriction of microbial growth and host disease resistance (1–3). Regulation of PAMP signaling responses must be tightly controlled because in eukaryotes, impaired growth and development has been linked to constitutive activation of immune responses (3, 4). Components contributing to attenuation of immune responses remain largely undefined in any organism.

Originally isolated as an *Arabidopsis thaliana* mutant with defects in stomatal cytokinesis, mutations in *SCD1* affect polarized cell expansion and cytokinesis of various epidermal cells (5). *SCD1* is implicated in overall plant growth and development because *scd1* mutants exhibit impaired aerial tissue growth, root elongation, flower morphogenesis, and sterility. In *Arabidopsis*, *SCD1* is a unique gene encoding for the only protein containing a complete DENN (Differentially Expressed in Normal and Neoplastic cells) domain (5), a tripartite protein motif that is conserved between animals and plants (6). Although the molecular function of the DENN domain remains largely undefined in most organisms, the DENN domain may confer guanidine exchange factor activity (7, 8). In animals, DENN domain-containing proteins are implicated in a variety of cellular pathways due to the presence of additional protein domain(s) that provide functional diversity (6, 9–11). Similarly, SCD1 contains eight tryptophan-aspartic acid (WD)-40 repeats (5), possibly coordinating multiprotein complex assembly (12). Our previous study on the *scd1-1* mutant demonstrates that the DENN domain is critical for SCD1 function. In *scd1-1* plants, a point mutation in a serine residue (S131F) that is highly conserved among eukaryotic DENN domains results in conditional defects in growth and development (5). These defects can be alleviated by shifting *scd1-1* plants from non-permissive (22 °C) to permissive temperature (16–18 °C) (5). *scd1-2* plants, a loss-of-expression T-DNA insertion line that exhibits more severe phenotypic defects compared with *scd1-1*, do not display the

* This work was supported in part by start-up funds from the University of Missouri (to A. H.), MU-Life Sciences Undergraduate Research Opportunity Program (to D. A. K. and K. A. W.), Human Frontiers of Science Program Grant (RGP22/2006) (to J. C. A.), and the National Science Foundation, Division of Molecular and Cellular Biosciences (0446157) (to S. Y. B.).

[S] The on-line version of this article (available at http://www.jbc.org) contains supplemental Figs. S1–S3 and Table S1.

[1] Present address: Monsanto Company, 800 N. Lindbergh Blvd., St. Louis, MO 63141.

[2] To whom correspondence should be addressed: Division of Biochemistry, University of Missouri-Columbia, 117 Schweitzer Hall, Columbia, MO 65211. Tel.: 573-882-3831; Fax: 573-882-5635; E-mail: heesea@missouri.edu.

[3] The abbreviations used are: PAMP, pathogen-associated molecular pattern; SCD1, stomatal cytokinesis-defective 1; DENN, differentially expressed in normal and neoplastic cells; PR, pathogen-related; cpr, constitutive expressor of PR; SA, salicylic acid; FLS2, flagellin-sensitive 2; PF22, active flg22; AF22, inactive flg22; LC-MS/MS, liquid chromatography-tandem mass spectrometry; WT, wild-type; qRT-PCR, quantitative real-time polymerase chain reaction; ROS, reactive oxygen species; MAPK, mitogen-activated protein kinase; Pst, *P. syringae* pathovar *tomato*; SID2, salicylic acid induction-deficient 2; CPN1/BON1, copine/bonzai; DAB, 3,3-diaminobenzidine; GST, glutathione *S*-transferase.

TABLE 1
PCR primers and gene loci

Primer name	Locus	5′-forward primer-3′	5′-reverse primer-3′
SCD1	*At1g49040*	ATATGGGATATTCGTTCAGGAAAGC	ACTCTTGCTGTCCAGTCATCACTTC
PR1	*At2g14610*	GGAGCTACGCAGAACAACTAAGA	CCCACGAGGATCATAGTTGCAACTGA
PR2	*At3g57260*	CGGTACATCAACGTTGGAA	GCGTAGTCTAGATGGATGTT
PR5	*At1g75040*	CGGTACAAGTGAAGGTGCTCGTT	GCCTCGTAGATGGTTACAATGTCA
LOX2	*At3g45140*	GTCCAAACCTCAGAAGACGAT	CACCCATGACTCACATGTAA
ERF2	*At5g47220*	AAGTGTGAGGTTGGTGATGAGACAC	GGTGCCTCAACATTTATAGCAAAAC
WRKY11	*At4g31550*	CCACCGTCTAGTGTAACACTCGAT	TGCAACGGAGCAGAAGCAAGGAA
WRKY33	*At2g38470*	AGCAAAGAGATGGAAAGGGGACAA	GCACTACGATTCTCGGCTCTCTCA
WRKY40	*At1g80840*	TGCGAGTTGAAGAAGATCCACCGA	TCCGAGAGCTTCTTGTTCTCAGCA
WRKY53	*At4g23810*	TTTGCCGATGGAGGAGGTTCTAGC	GCCTCTCTCTCTGGGCTTATTCTCAC
GAPDH 5′	*At1g13440*	TCTCGATCTCAATTTCGCAAAA	CGAAACCGTTGATTCCGATTC
GAPDH 3′	*At1g13440*	TTGGTGACAACAGGTCAAGCA	AAACTTGTCGCTCAATGCAATC
SAND family	*At2g28390*	AACTCTATGCAGCATTTGATCCACT	TGATTGCATATCTTTATCGCCATC
SCD1–393	*pGEX4T-1TEV*	CATGGATCCATGGGACGGATCTTCGAGTACTTC	
SCD1–391	*pGEX4T-1TEV*		ATAGCGGCCGCACAAAGAAAAAGTTGTGGAAGACAT
sid2-2 sm108	*At1g74710*	TTCTTCATGCAGGGGAGGAG	
sid2-2 sm30	*At1g74710*	CAACCACCTGGTGCACCAGC	
sid2-2 L1849	*At1g74710*		AAGCAAAATGTTTGAGTCAGCA
SCD1–545	*At1g49040*	AAGACTCTGTCTTTTCCGGGAGT	
SCD1–382	*At1g49040*		CTGTGGTGGGTGATCTCTTACTG

temperature sensitivity (5). The molecular mechanism(s) leading to any defects in these *scd1* mutant lines, however, are currently unknown.

Here, we show that in conditional *scd1-1* plants, the DENN mutation affected SCD1 protein accumulation in a temperature-dependent manner. Making use of the less severe growth defective phenotype compared with *scd1-2*-null mutant plants and the temperature-sensitive nature of *scd1-1* DENN (S131F), we provide evidence that in addition to its role in plant growth and development, SCD1 functioned in immune responses against bacteria. *scd1-1* also showed constitutive activation of defense responses, but *scd1-1* differed from previously described mutants displaying *cpr*-like phenotypes. Defects in *scd1-1* growth and development were genetically independent of salicylic acid (SA)-mediated signaling and could be uncoupled from constitutive activation of defense responses.

EXPERIMENTAL PROCEDURES

Plant Materials, Growth, and PAMPs—Seedlings or plants were grown at indicated temperatures and elicited with active flg22 (PF22; QRLSTGSRINSAKDDAAGLQIA) derived from *Pseudomonas aeruginosa*, inactive flg22 (AF22; ARVSSGLRVGDASDNAAYWSIA) derived from *Agrobacterium tumefaciens* or elf26 (SKEKFERTKPHVNVGTIGHVDHGKTT) as described (13) at indicated concentrations and times. *scd1-1* was in Col*gl1* background; *scd1-2*, *sid2-2*, and *bon1-1* were in Col0 background (5, 14, 15).

Genotyping—Genotyping was done using standard PCR techniques with indicated primers (Table 1). Cleaved amplified polymorphic sequence (CAPS) analysis was used to confirm the *scd1-1* point mutation. A fragment spanning the *DENN* point mutation was PCR amplified using *SCD1* primers SCD1–545 and SCD1–382 (Table 1) and directly subjected to restriction enzyme digest using BsmAI for subsequent CAPS analysis.

Production and Affinity Purification of αSCD1^{DENN} Antibodies—A 1822 bp *SCD1^{DENN}* fragment was PCR amplified using SCD1–393 and SCD1–391 primers (Table 1) and *SCD1* cDNA (5) as template, subcloned into a modified pGEX4T-1TEV vector (16) and verified by sequencing. Bacterially-expressed GST-SCD1^{DENN} fusion protein were solubilized from inclusion bodies and used for GST-SCD^{DENN} polyclonal antiserum production in rabbits using standard procedures. For affinity purification of SCD1^{DENN} antibodies, serum was first cleared of GST-specific antibodies by incubating the serum overnight with GST cross-linked to Affi-Gel 10 according to the manufacturer's instructions (Bio-Rad) and subsequently strip affinity-purified against solubilized GST-SCD1^{DENN} fusion protein resolved on preparative SDS-PAGE and transferred onto nitrocellulose membranes.

Immunoblot Analysis—Immunoblot analysis of total proteins was done as described (13) using antibody concentrations: αSCD1, 1:1200; αFLS2, 1:3000; αMPK6, 1:3000; αcalnexin (1:3000); αphospho-44/42 MAPK (αP-MAPK^{act}, Antibody #9101, 1:3000; Cell Signaling Tech., Danvers, MA).

Apoplastic ROS Production and MAPK Activation—Apoplastic ROS production and MAPK activation assays were performed as described (13) at indicated PAMP concentrations, times, and temperatures.

Seedling Growth Inhibition and Callose Deposition—Seedling growth inhibition and callose deposition assays were done as described (17) at indicated PAMP concentrations, times, and temperatures except in callose assays, seedlings were fixed and cleared in 95% ethanol.

DAB Staining—For detection of whole cell H_2O_2 (apoplastic and intracellular H_2O_2), DAB staining was done as described (18, 19) with the following modifications. Excised leaves of 4–5-week-old plants were vacuum infiltrated with 1 mg/ml DAB (3,3-diaminobenzidine; Sigma) and cleared by boiling in lactic acid/glycerol/EtOH (1:1:3) for 5–10 min.

Bacterial Pathogen Assays—Bioluminescent LuxCDABE-tagged *Pseudomonas syringae* pv. tomato DC3000 (20) were grown for 3 days on King's B Medium plates with appropriate antibiotics at 28–30 °C and resuspended in water to an OD of 0.005. Leaves of 4–5-week-old plants were syringe infiltrated with bacterial inoculums of 5×10^5 cfu/ml and left to dry. In bacterial plate assays, leaf discs were harvested at 0 and 3 dpi and ground in 10 mM $MgCl_2$. The cfu/cm^2 was determined by plating serial dilutions of individual leaf extracts. To monitor bacterial growth *in planta*, luciferase signal from bioluminescent *Pst* DC3000 was

detected in whole plants using a Photek HRPCS4 photon detection camera (21).

Quantitative Real-time PCR (qRT-PCR) Analysis—For elicited leaf samples, indicated PAMP concentrations were leaf syringe-infiltrated for indicated times. Seedlings (9-day-old) or leaf disks (from 4–5-week-old plants) were frozen in liquid nitrogen. Total RNA was extracted from frozen tissues and subjected to qRT-PCR reaction as described (22) with primers listed in Table 1. The expression of *At2G28390* (*SAND* family protein gene) was used to normalize all qRT-PCR results because of its highly stable expression during defense responses (22).

Statistical Analysis—Statistical analysis was performed using unpaired two sample *t* tests.

RESULTS

In plants, the bacterial PAMP flagellin or its active peptide derivative flg22 (PF22) is perceived by Flagellin-Sensitive 2 (FLS2) (1, 2). Previously, we employed a large-scale co-immunoprecipitation strategy using an αFLS2 antibody to discover novel PF22-dependent signaling component(s) required for innate immunity against bacteria (13). Here, we used the same approach to identify a protein with an apparent molecular mass of about 140 kDa that immunoprecipitated with the αFLS2 antibody in a PF22-independent manner from solubilized microsomal membranes of *La-er* cell culture (supplemental Fig. S1). Based on liquid chromatography-tandem mass spectrometry (LC-MS/MS) analysis, this protein was identified as SCD1 (supplemental Table S1), a DENN-domain containing protein required for growth and development (5). Probing αFLS2 immunoprecipitates with a purified polyclonal antibody made against the SCD1 DENN domain provided additional support that the identified 140 kDa protein was SCD1 (supplemental Fig. S2). Recent studies identified proteins with dual roles in development and innate immunity (1, 13, 23, 24). We therefore were interested in whether in addition to growth and development, SCD1 has role(s) in innate immunity, a function currently not ascribed to any eukaryotic DENN protein.

scd1-1 Is a Conditional Temperature-sensitive, Partial Loss-of-function Mutation—Prior to testing *SCD1* function in innate immunity, we investigated whether we could exploit the less severe growth defects and the temperature-sensitive nature of *scd1-1* relative to *scd1-2* (Fig. 1, *A* and *B*) (5) for subsequent assays. To gain a better understanding of the molecular mechanism(s) leading to the differences in phenotypic severity between these *scd1* mutants (5), we compared *SCD1* mRNA and protein levels between *scd1-1* and *scd1-2* grown at 22 °C. In *scd1-2*, no *SCD1* mRNA (Fig. 1*C*) or SCD1 protein (Fig. 1*D*; see also supplemental Fig. S3) was detected using qRT-PCR or immunoblot analysis with the αSCD1 antibodies, respectively. In contrast, phenotypic defects in *scd1-1* were not due to changes in *SCD1* mRNA accumulation (Fig. 1*C*) (5), but correlated with changes in SCD1 protein levels compared with wild type (WT). Long exposure of immunoblots showed reduced but detectable levels of SCD1 protein in *scd1-1* (Fig. 1*D*; see also supplemental Fig. S3). Thus, DENN integrity may be important for proper SCD1 stability or folding as recently suggested for RME-4, a DENN protein from *Caenorhabditis elegans* (11).

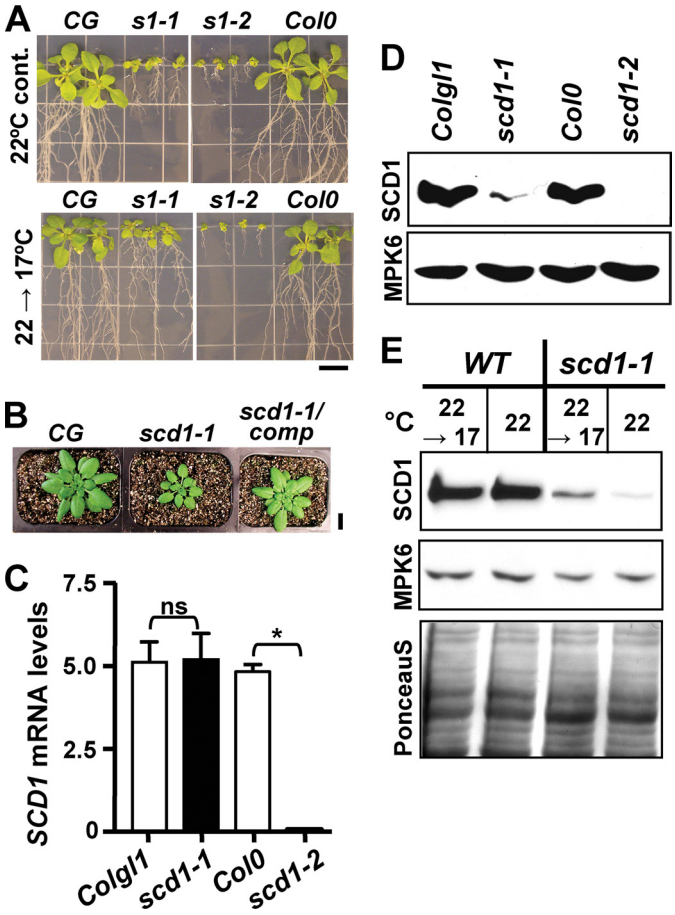

FIGURE 1. **SCD1 mRNA and protein accumulation in the temperature-sensitive mutant *scd1-1* and the null mutant *scd1-2*.** *A*, growth of *scd1* mutants after temperature shift experiments from non-permissive (22 °C) to permissive (17 °C) temperatures. *scd1-1* (*s1-1*), *scd1-2* (*s1-2*), and their WT (Col*gl1* and Col0, respectively) seedlings were grown on Murashige and Skoog plates containing 0.8% sucrose (MS plates) at 22 °C for 9 days. Seedlings were grown on MS plates for an additional 9 days at 17 °C (22 → 17 °C) or 22 °C (*cont.*). *B*, after growth on MS plates for 9 days, WT (*Colgl1*), *scd1-1*, and *scd1-1* complemented with *pSCD1::SCD1* (*scd1-1/comp*) seedlings were grown in soil for an additional 4 weeks. All growth was at 22 °C. *C*, *SCD1* mRNA expression levels. Total RNA isolated from *scd1* mutants and WT were used as templates for qRT-PCR using *At2g28390* as a reference gene. Samples ($n = 5–6$) were analyzed for each plant line. Statistical (*asterisks*) and non-statistical (*ns*) significance are shown. ± indicates S.E. *D*, SCD1 protein accumulation in *scd1* mutants. Total proteins were subjected to immunoblot analysis using αSCD1-DENN or αMPK6 (loading control) antibodies. *E*, increase in SCD1 protein accumulation in *scd1-1* mutants after temperature shift from 22 to 17 °C. 7-day-old seedlings grown at 22 °C were shifted for 4 days to 17 °C or kept at 22 °C. Total proteins were subjected to immunoblot analyses using αSCD1-DENN antibody. PonceauS staining and αMPK6 antibodies were used as loading controls. Unless stated otherwise, 9-day-old seedlings grown at 22 °C were used. All experiments were done three times. *Bars*, 1 cm.

scd1-1 seedlings grown at non-permissive (22 °C) and transferred for 4 days to permissive (17 °C) temperature consistently accumulated more SCD1 protein relative to *scd1-1* grown continuously at 22 °C, but did not reach levels found in WT (Fig. 1*E*). Increased SCD1 protein levels correlated with alleviation of phenotypic defects upon temperature shift to 17 °C (Fig. 1*A*) (5). We conclude that *scd1-1* is a conditional temperature-sensitive, partial loss-of-function mutation whereas *scd1-2* is a complete loss-of-function mutation.

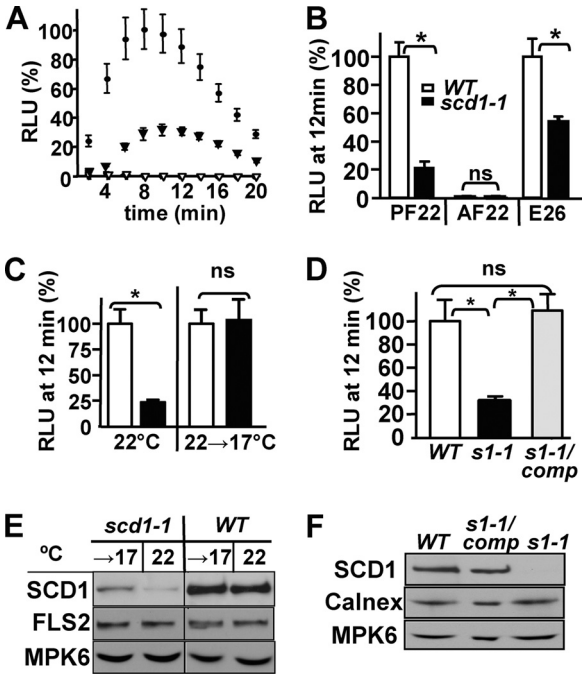

FIGURE 2. **Impaired PF22-elicited ROS response in conditional *scd1-1*.** *A*, ROS production in minutes (min) in expanded leaves of *scd1-1* (*triangle*) compared with the WT Col*gl1* (CG, *circle*) in response to 10 nM PF22 (*filled*) or DMSO (*open*). ROS production ($n = 6–7$) was shown as relative light units (RLU) in percent (%) relative to PF22-induced WT. *B*, ROS production in response to other bacterial PAMPs. ROS production was shown as RLU at maximum induction (12 min) after elicitation with 10 nM PF22, AF22, or elf26 (E26) in *scd1-1* (*black bar*) and *WT* (*white bar*). Experiments ($n = 5–6$) were done twice (AF22) or at least three times (PF22 and E26). *C*, temperature shift to 17 °C alleviated impaired PF22-ROS production in *scd1-1*. After growth at 22 °C, mature plants were shifted for 9 days to permissive (22 → 17 °C) or kept continuously (22 °C) at 22 °C. ROS production ($n = 5$) for *scd1-1* (*s1-1; black*) and *WT* (*white*) was shown as in *B* after 10 nM PF22 elicitation. *D*, complementation of ROS defects in *scd1-1* transformed with *pSCD1::SCD1*. ROS production in leaf tissue ($n = 6–8$) was shown after 10 nM PF22 elicitation in *scd1-1* (*s1-1*; *black bar*), *WT* (*white bar*), and *scd1-1/pSCD1::SCD1* (*s1-1/comp*; *gray bar*) as RLU at maximum induction (12 min). *E*, increased SCD1 protein accumulation after temperature shift from 22 to 17 °C. Leaf disks were taken from the same plants used in *C*. Total proteins were subjected to immunoblot analyses using αSCD1-DENN and αFLS2 antibodies. Blots probed with αMPK6 antibodies showed equal loading. *F*, *scd1-1* plants transformed with *pSCD1::SCD1* expressed SCD1 protein to WT levels. Leaf disks were taken from the same plants used in *D*. Total proteins were probed in immunoblot analysis with αSCD1-DENN. Blots probed with αMPK6 (cytosolic) and αcalnexin (ER) antibodies showed equal loading. Unless stated otherwise, plants were grown at 22 °C, and experiments done at least three times, all with similar results. Statistical (*asterisks*) and non-statistical (*ns*) significance are indicated. ± indicates S.E.

Conditional scd1-1 Show Impaired PAMP-induced ROS Responses—To investigate SCD1 function in innate immunity, we focused on *scd1-1*. In contrast to *scd1-2* (5), *scd1-1* grew sufficiently at 22 °C for experimental manipulation (Fig. 1*B*). First, we tested whether *SCD1* has a genetic role in PF22-dependent signaling responses. As determined by luminol-based assays (17), PF22-elicited rapid and transient accumulation of apoplastic (extracellular) reactive oxygen species (ROS) in small leaf pieces of 4–5-week-old WT plants (Fig. 2, *A* and *B*). At 22 °C, PF22-elicited ROS production was significantly reduced in *scd1-1* leaves compared with WT at each time point (Fig. 2, *A* and *B*; $p \leq 0.0013$), indicating a role for SCD1 in PF22-induced oxidative burst. In control experiments, no ROS were produced in response to DMSO or inactive flg22 (AF22) in *scd1-1* or WT (Fig. 2, *A* and *B*). *scd1-1* plants also displayed significantly impaired ROS production in response to elf26 (Fig. 2*B*; $p < 0.005$), a bacterial PAMP structurally unrelated to PF22 and perceived by an independent PAMP receptor, EFR (25). Thus, SCD1 function was not restricted to PF22-elicited ROS production.

To confirm that impaired PF22-induced ROS production was caused by the DENN mutation in *SCD1*, *scd1-1* plants were grown at 22 °C continuously or shifted from 22 to 17 °C for 9 days. In contrast to ROS defects in *scd1-1* grown at 22 °C, no significant difference was observed in PF22-induced ROS production between *scd1-1* and WT plants shifted to 17 °C (Fig. 2*C*). Thus in addition to alleviating growth and developmental defects (5), a shift from 22 to 17 °C restored a molecular phenotype, namely PF22-induced ROS production in *scd1-1*. Reversal of the ROS defect in *scd1-1* correlated with increased SCD1 protein levels (Fig. 2*E*), but these did not reach WT levels. No discernible change in SCD1 protein accumulation was observed in WT plants when grown at 22 °C and shifted to 17 °C. In addition, FLS2 protein levels were similar in *scd1-1* and WT plants independent of growth conditions (Fig. 2*E*; see also supplemental Fig. S3). Transformation of *scd1-1* with the *SCD1* gene under the control of its own promoter (*scd1-1/pSCD1:SCD1*; *scd1-1/comp*) complemented the phenotypic defects of *scd1-1* plants (Fig. 1*B*) (5) at 22 °C and restored SCD1 protein accumulation to WT levels (Fig. 2*F*). Importantly, expression of WT SCD1 protein restored the ROS defect in *scd1-1* plants (*scd1-1/pSCD1:SCD1; s1-1/comp*; Fig. 2*D*). Taken together, we showed by two independent means (temperature shift and complementation assays) that reduced PF22-ROS production was due to the DENN point mutation in *SCD1*.

SCD1 Function Is Required for Some but Not All flg22 Responses—Next we investigated whether *SCD1* was required for other early or late PF22-responses when grown at the non-permissive temperature (22 °C). Previously, seedling growth inhibition assays were successful in identifying components of PAMP signaling pathways by assessing seedling sensitivity to bacterial PAMPs (17, 25). Here, 4-day-old seedlings were subsequently grown in the presence of active (PF22, elf26) or inactive (AF22) PAMPs for additional 7 days. Based on weight measurements of individual seedlings, WT exhibited dose-dependent growth reduction in the presence of PF22 (expressed in percentage relative to seedlings grown in AF22) (Fig. 3*A*). At the same PF22 concentrations, *scd1-1* seedling growth was significantly less inhibited indicating a reduced sensitivity of *scd1-1* to PF22 (Fig. 3*A*; $p < 0.0001$). Reduced sensitivity was not due to a limitation of *scd1-1* seedlings to be further stunted because exposure to 1 μM elf26 (E26), a more potent PAMP in this assay compared with PF22, resulted in increased growth inhibition of *scd1-1* seedlings (Fig. 3*A*). Taken together, these results implicate a role of *SCD1* in seedling growth inhibition to bacterial PAMPs.

To further examine the requirement for SCD1 in early and late PAMP responses, we determined PF22-induced transcriptional activation of a subset of early marker genes (26) in leaves of 4–5 week old plants after syringe-inoculation with PF22 or a mock control (DMSO) for 30 min. As determined by qRT-PCR, transcript accumulation of tested WRKY transcription factors, previously shown to be up-regulated in response to flg22 (26),

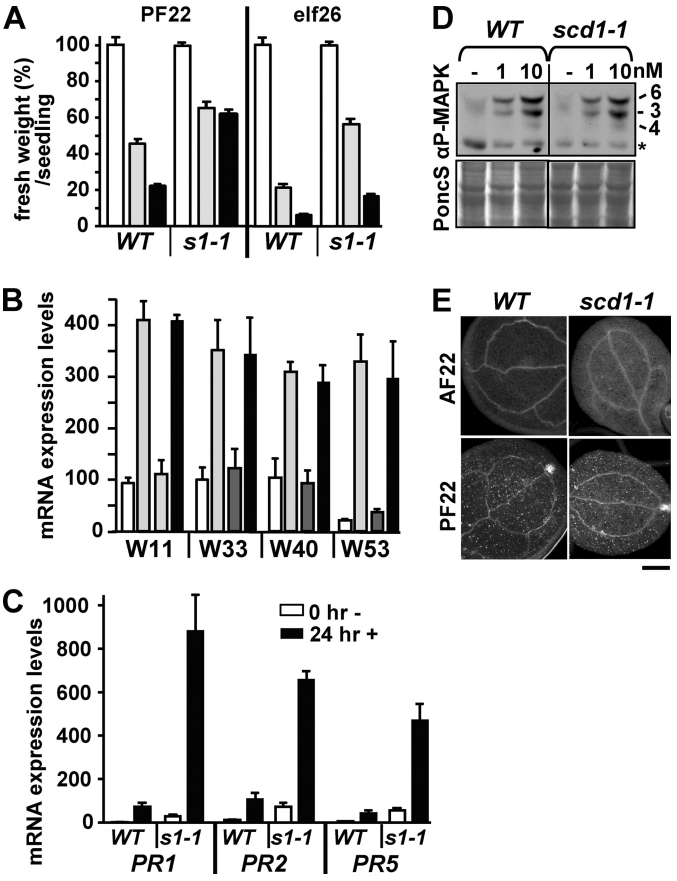

FIGURE 3. **SCD1 was required for a subset of PF22 signaling responses at 22 °C.** *A*, impaired seedling growth inhibition in *scd1-1* in response to PAMPs. 4-day-old *scd1-1* (*s1-1*) and WT seedlings were transferred to MS medium containing PAMPs at the following concentrations: 1 μM AF22 (*white bars*), 0.1 μM PF22 or elf26 (*gray bars*), and 1 μM PF22 or elf26 (*black bars*). After 7-day treatment, fresh weight of individual seedlings ($n = 10$) was measured and calculated in percentage (%) relative to AF22 treatment (100%). *B*, PF22-induced transcript accumulation of tested *WRKY* (*W*) transcription factor genes was not impaired in *scd1-1*. Leaves of 4-week-old plants were syringe-infiltrated with DMSO (WT, *white*; *scd1-1*, *dark-gray*) or 0.1 μM PF22 (WT, *light gray*; *scd1-1*, *black*). After 30 min, leaf disks ($n = 3–4$) were taken and processed for qRT-PCR using *At2g28390* as the reference gene. *C*, PF22 elicitation led to increased transcript accumulation of *PR1*, *PR2*, and *PR5* in *scd1-1*. Leaves of 4-week-old plants were syringe-infiltrated with 0.1 μM PF22. At 0 h (*white*) or after 24 h (*black*), leaf disks ($n = 3–4$) were taken and processed as described in *B*. *D*, PF22-induced MAPK activation was not impaired in *scd1-1*. 8-day-old *scd1-1* and *WT* seedlings were treated for 10 min with 1 or 10 nM PF22 or DMSO (−). Total proteins were subjected to immunoblot analysis using an α-phospho44/42-ERK antibody (αP-MAPK^{act}). MPK6 (6), MPK3 (3), and MPK4 (4) were identified by mass. A cross-reacting protein band (*asterisk*) and PonceauS (*PoncS*) staining served as loading control. *E*, PF22-induced callose deposition was not impaired in *scd1-1* seedlings. 8-day-old WT and *scd1-1* seedlings were treated with 0.1 μM PF22 or AF22 for 24 h. Seedlings were stained with aniline blue to visualize callose deposition as *tiny bright dots*. *Bar*, 0.5 mm. Plants and seedlings were grown at 22 °C. Experiments were done at 22 °C at least three times. ± indicates S.E. WT is Col*gl1*.

were increased after PF22 elicitation compared with mock-treated tissue. WT and *scd1-1* plants showed no statistically significant differences in induction of these marker transcripts (Fig. 3*B*). Similar results were obtained from PF22-treated 9-day-old seedlings. We also investigated transcript accumulation of pathogen-related *(PR) PR1*, *PR2*, and *PR5* genes, known late marker genes for PF22 signaling and defense responses (17, 27). Interestingly, PF22 elicitation for 24 h led to a significant increase in transcript accumulation of *PR1*, *PR2*, and *PR5* genes in *scd1-1* compared with WT leaves (Fig. 3*C*; $p < 0.001$). These results implicated *SCD1* as a negative regulator of PF22-induced transcript accumulation of these marker *PR* genes.

Next, we determined whether PF22-dependent activation of mitogen-activated protein kinases (MAPKs) MPK3, MPK6, and MPK4, generally used to monitor early PAMP responses (2), was affected in *scd1-1*. After elicitation with increasing PF22 concentrations for 10 min, we did not observe any differences in the activation of these MAPKs when comparing *scd1-1* and WT seedlings (Fig. 3*D*) using an antibody (αP-MAPK^{act}) that detects activated, phosphorylated MAPKs (13). Finally using a classical assay for late PAMP responses (17), we examined PF22-induced callose deposition in seedlings. PAMP elicitation induces synthesis of callose, a β-1,3-glucan polymer visualized as tiny bright dots by aniline blue staining (2, 17). After elicitation with PF22 for 24 h, *scd1-1* seedlings showed callose deposition similar to WT (Fig. 3*E*) indicating that PF22-induced callose accumulation was independent of the *SCD1 DENN* mutation. In control experiments, no callose accumulation was observed in *scd1-1* or WT seedlings in the absence of any treatment or in response to inactive flg22 (AF22; Fig. 3*E*). Taken together, *SCD1* was required for some (ROS production, seedling growth inhibition, transcript accumulation of *PR1*, *PR2*, *PR5* genes) but not other PF22-elicited signaling responses (transcript accumulation of tested *WRKY* genes, activation of MAPKs, callose deposition).

scd1 DENN Mutation Leads to Constitutive Activation of Defense Responses and Increased Basal Resistance Against Bacteria—During gene expression profiling of plant material grown at 22 °C, we observed increased transcript accumulation of *PR* genes in *scd1-1* seedlings and leaves compared with WT in the absence of any PAMP elicitation (Fig. 3*C*; data not shown). *PR1* is a defense marker gene for SA-regulated signaling responses whose expression is induced after PAMP treatment or pathogen infection (4, 28). Plant mutants showing constitutive expression of *PR1* gene in the absence of any stimulus are categorized as *cpr* (*c*onstitutive expressor of *PR*) mutants (4). In general, *cpr* mutants exhibit constitutive activation of defense responses as exemplified by aberrant expression of hormone-inducible defense genes, activation of callose deposition and whole cell accumulation of H_2O_2 in the absence of any stimulus (18, 29–32).

Thus, we tested next whether non-treated *scd1-1* displayed additional *cpr*-like phenotypes. We focused first on transcript accumulation of other hormone-inducible genes involved in defense responses using qRT-PCR analyses. Non-treated *scd1-1* leaves accumulated statistically significant higher mRNA levels of the SA-marker genes *PR1*, *PR2*, and *PR5* compared with WT (Figs. 3*C* and 4*A*; $p \leq 0.01$). In contrast, mRNA levels of marker genes (*LOX2* and *EFR2*) for jasmonic acid and ethylene, hormones with antagonistic immune response function to SA (28), were significantly reduced in *scd1-1* compared with WT (Fig. 4*A*; $p \leq 0.01$). Thus, *scd1-1* showed aberrant regulation of hormone-inducible defense genes in the absence of any stimulus.

As described earlier, when examining callose deposition at the seedling stage (7–9-day-old), *scd1-1*, or WT did not display any significant callose accumulation in the absence of active PAMP treatment (see AF22; Fig. 3*E*). At a later stage of devel-

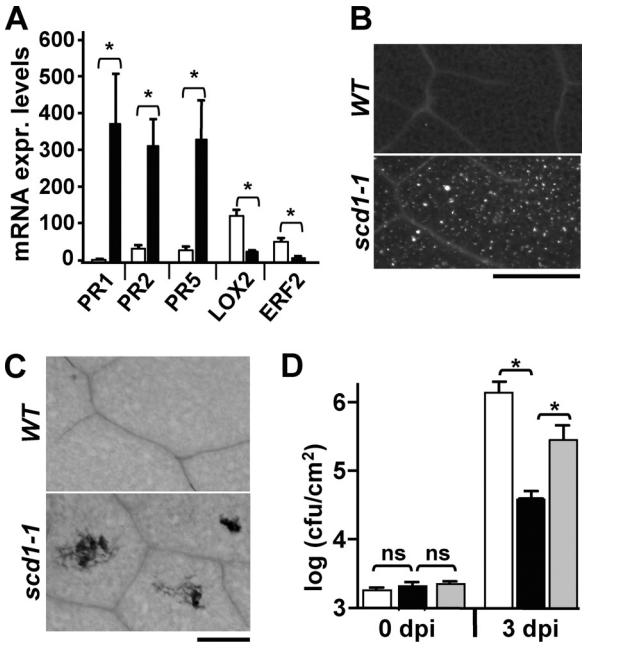

FIGURE 4. **Mature *scd1-1* leaves showed constitutive activated defense responses and increased basal resistance against *Pst* DC3000 at 22 °C.** *A*, aberrant hormone-inducible gene expression in non-treated *scd1-1* (*black bars*) compared with WT (*white bars*). Leaf disks were processed for qRT-PCR with *At2g28390* as a reference gene. Samples from 3–4 independent experiments were analyzed for each plant line. *B*, increased callose deposition in untreated *scd1-1* leaves. Leaves of non-treated plants were stained with aniline blue to visualize callose. Experiments were done three times for 3–4 leaves taken from 3 different *scd1-1* or WT plants. *Bar*, 0.5 mm. *C*, H_2O_2-stainable lesions in untreated *scd1-1* leaves. Leaves of non-treated plants were stained with DAB to visualize H_2O_2-stainable lesions. Experiments were done twice for 3–4 leaves taken from three different *scd1-1* or WT plants. *Bar*, 0.2 mm. *D*, increased bacterial resistance to *Pst* DC3000 in *scd1-1*. Leaves of *scd1-1* (*black bars*), *WT* (*white bars*), and *scd1-1/pSCD1::SCD1* (*scd1-1/comp*; *gray bars*) plants were syringe-infiltrated with 5×10^5 *Pst* DC3000. At 0 and 3 days post-infiltration (dpi), bacterial growth was assessed in leaf disks ($n = 10–12$) from individual leaves of three independent plants using bacterial plate assays. Experiments were performed 2–3 times. No statistical difference, *ns*; colony forming units per cm^2, cfu/cm^2. *Asterisk* indicates statistically significant differences. Plants were grown, and experiments were performed at 22 °C. ± indicates S.E. WT is Col*gl1*.

opment, however, we observed increased callose deposition in 4–6-week-old untreated *scd1-1* leaves compared with WT (Fig. 4*B*). Non-treated *scd1-1* leaves also showed increased H_2O_2 stainable lesions compared with WT (Fig. 4*C*) as determined by DAB staining, a technique commonly used to detect whole cell H_2O_2 produced at high magnitude during the hypersensitive response (HR) or cell death (18, 19). DAB is taken up by living plant tissue cells, thus enabling detection of intracellular H_2O_2 produced by organelles (19). Because in non-elicited *scd1-1* leaves, we did not detect increased levels of apoplastic (extracellular) ROS using the sensitive luminol-based ROS assay, (Fig. 2, *A* and *B*; *DMSO* and *AF22*), DAB staining in non-elicited *scd1-1* leaves is likely due to increased levels of intracellular H_2O_2. These results together indicate that in the absence of any PAMP treatment or pathogen infection, *scd1-1* exhibited constitutive activation of defense response phenotypes that are generally associated with *cpr* mutants.

cpr mutants are known to show increased basal resistance against bacteria (30, 32). Thus, we investigated whether growth of a *P. syringae* pathovar *tomato* (*Pst*) DC3000 strain was affected in *scd1-1* plants. Because open stomata provide entry ports for invading bacteria (33), we syringe-infiltrated (as opposed to spray-inoculation) mature leaves with 5×10^5 *Pst* DC3000 to eliminate any possible effect on bacterial growth due to the reduced number of functional stomata in *scd1-1.* Using bacterial plating assay, no statistical difference in bacterial growth (cfu/ml) was observed between *scd1-1* and WT leaves at 0 dpi (Fig. 4*D*). But after 3dpi, growth of *Pst* DC3000 was significantly reduced in *scd1-1* leaves by more than 10-fold compared with WT (Fig. 4*D*; $p < 0.0001$; see also Fig. 5, *C* and *D*). These results implicated SCD1 genetically as a negative regulator of basal resistance against *Pst* DC3000. In control experiments, *scd1-1* plants expressing the *SCD1* gene under the control of its own promoter (*scd1-1*/comp) complemented bacterial growth repression at 3dpi (Fig. 4*D*; $p < 0.002$).

Growth and Developmental Impairments Can Be Uncoupled from Constitutive Activation of Defense Responses and Resistance Phenotypes in scd1-1—In eukaryotes, growth and developmental defects have been attributed to constitutive activation of immune responses (3, 15). In *cpr* mutants, these defects correlate with up-regulation of SA-dependent signaling (*i.e.* increased *PR1* transcript levels) and can be reversed genetically by introducing *SID2* (*Salicylic acid Induction-Deficient 2*) mutant alleles impaired in defense-related SA biosynthesis (14, 28). To test whether the *scd1-1* growth defect was SA-dependent, we generated homozygous *scd1-1sid2-2* double mutants. In these double mutants, *PR1* transcript accumulation was similar to WT levels indicating that *sid2-2* reversed the increased accumulation of *PR1* transcript present in *scd1-1* (Fig. 5*A*, $p \leq 0.001$). Furthermore, leaves of *scd1-1sid2-2* plants did not display increased callose deposition observed in *scd1-1* (Fig. 5*B*). Taken these data together (Fig. 5, *A* and *B*), *sid2-2* suppressed constitutive activation of defense responses observed in *scd1-1*.

Next, we investigated whether inhibition of defense-related SA biosynthesis genetically suppressed the increased resistance against bacteria observed in *scd1-1* plants (Figs. 4*A*, 5*C*, and 5*D*). To this end, *scd1-1* single and *scd1-1sid2-2* double mutant plants were syringe-infiltrated with a *Pst* DC3000 strain (5×10^5). WT (*Colgl1*) and *sid2-2* plants were used as controls. First, we determined changes in resistance phenotypes using bacterial plate assays (colony forming units (cfu)/cm^2). No significant difference of bacterial growth was observed between plant lines at 0 dpi indicating equal infiltration (data not shown; Fig. 4*D*). At 3dpi, *scd1-1sid2-2* double mutant plants were significantly more susceptible to bacterial infection than *scd1-1* and WT (Fig. 5*C*; $p < 0.0001$). More specifically, double mutant plants displayed increased bacterial growth to statistically similar levels as the *sid2-2,* a mutant known to have increased susceptibility to bacterial infection (14, 28). These results indicated that *sid2-2* suppressed the resistance phenotype of *scd1-1.*

In our studies, plants were infiltrated with *Pst* DC3000 carrying a chromosome insertion of the luxCDABE operon, a bioluminescent bacterial strain whose luminescence has been reported to accurately and reliably reflect bacterial growth in infected *Arabidopsis* leaves (20, 21). Using this bioluminescent bacterial strain enabled us to monitor growth of bioluminescent *Pst* DC3000 *in planta* using a Photek luminescent camera system (Fig. 5*D*). Importantly, results obtained with this camera system were consistent with those from the bacterial plate assay

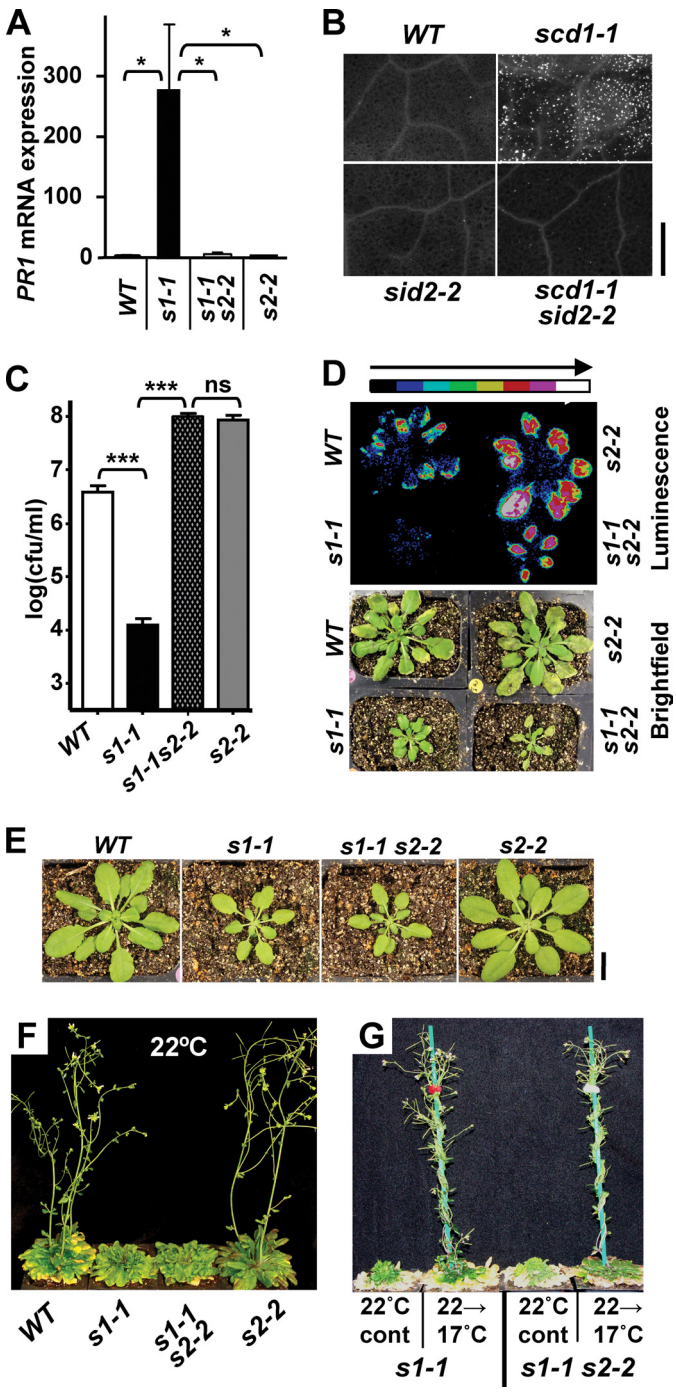

FIGURE 5. **Uncoupling of growth and developmental defects from constitutive defense response activation and resistance in *scd1-1*.** *A*, suppression of *PR1* transcript accumulation by *sid2-2* (*s2-2*) in *scd1-1sid2-2* (*s1-1s2-2*) double mutant. *PR1* transcript accumulation was determined using qRT-PCR with *At2g28390* as a reference gene. Samples ($n = 5$) from 2–3 independent experiments were analyzed for each line. *B*, suppression of callose deposition by *sid2-2* in the *scd1-1sid2-2* double mutant. Non-elicited leaves (4–5-weeks-old) were stained with aniline blue to show callose deposition. Experiments were done three times for 3–5 leaves taken from three different plants per plant line. *Bar*, 0.5 mm. *C*, suppression of increased resistance against LuxCDABE-tagged *Pst* DC3000 in *scd1-1* by *sid2-2* as shown by bacterial plate assay. Leaves of *scd1-1* (*black bar*), *WT* (*white bar*), *scd1-1sid2-2* (*gray hatched bar*) and *sid2-2* (*gray bar*) plants were syringe-infiltrated with 5×10^5 LuxCDABE-tagged *Pst* DC3000. At 3 days post-infiltration (dpi), bacterial growth was assessed in leaf disks ($n = 10–12$) from individual leaves of 3–4 independent plants. Experiments were performed 2–3 times. Colony forming units per cm^2, cfu/cm^2; *D*, suppression of increased resistance against LuxCDABE-tagged *Pst* DC3000 in *scd1-1* by *sid2-2* monitored by *in planta* growth of bioluminescent bacteria. Prior to processing plants for bacterial plate assay (*C*), plants were imaged at 3dpi by bright field or with a Photek camera to monitor *in planta* growth of bioluminescent bacteria. A representative plant is shown for each plant line. *Arrow* indicates increasing bioluminescence with cold colors (*blue*, *green*) or warm colors (*red*, *pink*, *yellow*, *white*) representing regions of lower or more intense regions of luminescence, respectively. *E*, no suppression of the *scd1-1* growth impairment by *sid2-2* in *scd1-1sid2-2* double mutant. *scd1-1* single and *scd1-1sid2-2* double mutants are progenies from the same cross. Plants were grown for 4 weeks at 22 °C. *Bar*, 1 cm. *F*, no suppression of the *scd1-1* flowering defect by *sid2-2* in *scd1-1sid2-2* double mutant. Plants were grown for 7 weeks at 22 °C. *G*, conditional flowering and sterility of the *scd1-1* single and *scd1-1sid2-2* double mutant plants. After growth at 22 °C for 2 months, plants were either kept at 22 °C (22 °C cont) or moved to 17 °C for an extra 2 months (22 → 17 °C). WT is *Colgl1*; *s1-1* is *scd1-1*; *s2-2* is *sid2-2*; *s1-1s2-2* is *scd1-1sid2-2* double mutant. Unless stated otherwise, plants were grown at 22 °C. *Asterisk(s)* indicates statistically significant differences. ± indicates S.E.

(Figs. 4*D* and 5*C*), in that (*a*) *scd1-1* plants showed reduced growth of luminescent bacteria compared with WT and (*b*) *sid2-2* showed increased bacterial growth compared with WT and *scd1-1* (Fig. 5*D*). Importantly, in agreement with plate assay results, *scd1-1sid2-2* plants supported increased bacterial growth compared with *scd1-1* and WT plants (Fig. 5*D*) indicating that *sid2-2* suppressed the resistance phenotype associated with *scd1-1*. Taken these results together (Fig. 5, *A–D*), we conclude that in *scd1-1*, both constitutive activation of defense responses and increased resistance against bacteria could be correlated genetically to defense-related SA biosynthesis.

We noted, however, that *sid2-2* was unable to rescue growth impairment of *scd1-1* because *scd1-1sid2-2* double mutants did not grow to larger size compared with *scd1-1* (Fig. 5*E*). Furthermore, *sid2-2* did not rescue the conditional flowering and sterility defects of *scd1-1* at 22 °C (Fig. 5*F*). Similar to the conditional, temperature-sensitive *scd1-1* (5), *scd1-1sid2-2* double mutant plants showed impairment in flower development and did not set seeds at 22 °C. Only after shift to permissive temperature (17 °C) did *scd1-1sid2-2* develop fertile flowers that produced siliques and seeds (Fig. 5*G*). Thus, in contrast to previously described mutants with *cpr* phenotypes (28), the growth and developmental defects in *scd1-1* plants were genetically independent (or upstream) of defense-related SA signaling pathway(s).

In *cpr*-like mutants, growth impairment and constitutive defense response activation can also be rescued by growing mutant plants at elevated temperatures as shown for plants with mutations in *copine/bonzai* (*CPN1/BON1*) (15, 32). In agreement, temperature shift from 22 °C to 28 °C for 9 days rescued *bon1-1* growth impairment and repressed constitutive transcript accumulation of *PR1* gene compared with *bon1-1* continuously grown at 22 °C (Fig. 6, *A* and *B*). In *scd1-1*, shift to 28 °C also suppressed elevated *PR1* transcript accumulation (Fig. 6*B*, $p \leq 0.001$). But in contrast to *bon1-1* and other mutants with *cpr*-like phenotypes (15, 18, 31, 34, 35), growth impairment of *scd1-1* was not rescued by shift to high temperature (Fig. 6*A*). These results provided additional evidence that growth and developmental defects of *scd1-1* could be uncoupled from constitutive activation of defense responses.

DISCUSSION

SCD1 is implicated in plant growth and development, likely due to its role in cytokinesis and polarized cell expansion (5).

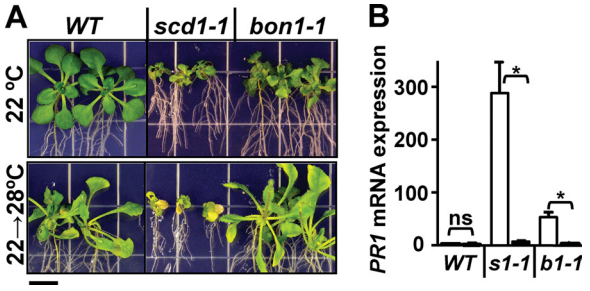

FIGURE 6. **Shift to high temperature did not suppress growth defect of *scd1-1*.** *A*, no suppression of growth impairment in *scd1-1* grown at 28 °C. After 9 days of growth at 22 °C on plates, seedlings were transferred for 9 more days to 28 °C or kept at 22 °C. Experiments were done at least 3 times for each line. *Bar*, 1 cm. *B*, suppression of *PR1* transcript accumulation by high temperature in *scd1-1*. Using plants from *A*, *PR1* transcript accumulation was determined using qRT-PCR as in Fig. 5*A*. *White bars* indicate seedlings kept continuously at 22 °C, *black bars* indicate seedlings shifted to 28 °C. Samples ($n = 4–6$) from 2–3 independent experiments were analyzed per line. Statistical differences (*asterisks*), non-significance (*ns*), and S.E. (±) are indicated. WT is Col*gl1*; *s1-1* is *scd1-1*; *b1-1* is *bon1-1*.

Here, we identified novel function(s) of *SCD1* in innate immune responses against bacteria, some of which were independent of a *SCD1* requirement in plant growth and development (Figs. 5 and 6). Thus, our study on SCD1 expands our limited knowledge on proteins with dual roles in innate immunity as well as growth and development (23, 24, 36).

We showed that the *DENN* mutation in *SCD1* affected some (ROS production, seedling growth inhibition, *PR* transcript accumulation; Figs. 2 and 3), but not other (activation of gene transcription and MAPKs, callose deposition; Fig. 3) PF22-elicited signaling responses. The fact that in *scd1-1*, a subset of PF22-responses was induced to WT levels at the restrictive temperature (22 °C) suggested that FLS2-function (*i.e.* in PF22 perception) was not impaired in these mutant cells. Furthermore, FLS2 protein levels were similar in *scd1-1* and WT plants independent of growth conditions (Fig. 2*E* and supplemental Fig. S3). These results indicate that in *scd1-1*, (*a*) the PF22-signaling defects at 22 °C were not due to overall reduced FLS2 receptor levels and (*b*) in temperature shift experiments to 17 °C, reversal of the ROS defect was not due to increased FLS2 protein levels. Consistent with the notion that impairment of some PF22 responses could not be attributed to decreased FLS2 receptor levels, FLS2 protein levels were also not reduced in *scd1-2*-null mutant seedlings (supplemental Fig. S3).

It is possible that the *scd1-1* mutation may affect the function of PF22-signaling component(s) downstream of FLS2/PF22 perception. A potential candidate may be RbohD, the plant homolog of the mammalian gp91^{phox} respiratory burst NADPH-oxidase subunit required for PF22-induced rapid burst of extracellular ROS (37, 38). The observed PAMP defects of *scd1-1*, however, cannot be solely explained by impaired RbohD function. In contrast to *scd1-1*, *rbohD*-null mutants are impaired in PF22-induced callose deposition (38) (data not shown). Furthermore, *rbohD*-null mutants do not exhibit any obvious growth defects or any resistance defect after bacterial infection (39). Thus, SCD1 may exert its PF22 signaling function via yet unknown component(s). Another possible explanation for why only a subset of PAMP responses was affected in *scd1-1* may be the existence of parallel and/or multibranched PAMP signaling pathways rather than a single linear pathway (40).

In addition to functioning as a positive regulator of PAMP responses, our data also implicated *SCD1* as a negative regulator of PF22 signaling responses. In *scd1-1*, PF22 elicitation led to increased transcript accumulation of *PR1*, *PR2*, and *PR5* (Fig. 3*C*). Increased transcript accumulation of these SA-regulated defense marker genes may at least in part account for increased resistance against bacteria of *scd1-1*.

Furthermore, *scd1-1* plants displayed constitutive activation of defense responses and increased resistance against *Pst* DC3000 (Fig. 4) implicating *SCD1* genetically as a negative regulator of immune responses. These immune phenotypes are reminiscent of those described for *cpr* mutants. But in contrast to most previously described mutants with *cpr*-like phenotypes (15, 18, 31, 34, 35), *SCD1* has a role in plant growth and development *per se*. Using two independent approaches (blocking SA biosynthesis genetically by introducing the *sid2-2* mutant allele into *scd1-1* and shift to high temperature; Figs. 5 and 6), we provide evidence that conditional growth and sterility defects of *scd1-1* could be uncoupled from constitutive activation of defense responses and increased resistance to bacteria. We conclude that *SCD1* appears to function in multiple and diverse cellular pathways.

It remains to be determined whether the role(s) of *SCD1* as (*a*) a positive regulator of PAMP responses (ROS production, seedling growth inhibition), (*b*) a negative regulator of flg22-elicited *PR* transcript accumulation, and (*c*) a negative regulator of constitutive activation of defense responses and bacterial resistance are separate or interrelated functions. In support of the latter, recent studies (41, 42) suggest an interplay between PAMP-elicited and SA-mediated innate immune responses. Perhaps SCD1 may function in PAMP-induced activation of a yet unknown component that, in turn, may be required in attenuating SA-mediated defense responses. In this model, impaired PF22 activation of this component would lead to constitutive activation of defense responses and increased resistance against bacteria. This model is in agreement with a recent study (40) indicating that a significant element in mounting robust immunity involves sustained PAMP receptor signaling that induces and maintains transcriptional reprogramming at a relatively late phase (including that of *PR* genes).

We cannot, however, exclude the possibility that *SCD1* may have independent and possibly antagonistic functions as shown for *BAK1*. *BAK1* has dual roles as a positive regulator of PAMP responses (13, 24) and as a negative regulator of constitutive defense response activation (34). But in contrast to *SCD1*, *BAK1* function in constitutive activation of defense responses is linked to its role in plant growth and development (34).

Interestingly, the mammalian DENN domain protein DENN/MADD has dual roles in neuronal processes as a positive and negative regulator, and these functions are exerted through targeting different proteins. Interaction of DENN/MADD with tumor necrosis factor receptor 1 (TNFR1) suppresses signaling pathways that regulate neuronal cell death (9). DENN/MADD also functions in neurotransmission by positively regulating small GTPase Rab3 activities (10, 43). Ulti-

mately, reduced DENN/MADD levels impair overall growth and development (10, 44) and correlate with cell death and neurological diseases such as Alzheimer's (9, 45). To our knowledge, however, animal DENN protein function in innate immune responses has not been reported. Gaining further insight into the roles of *SCD1* in plant innate immunity and growth and development represents an exciting goal to advance our general understanding of DENN protein function in eukaryotes.

Acknowledgments—We thank Dr. Walter Gassmann for growth chamber space, discussion, and bon1-1 seeds; Dr. Scott Peck for MPK6 antibody and elf26; Dr. Jonathan Jones for Pst strain; Dr. Barbara Kunkel for sid2-2 seeds and discussion; Dr. Mary Wildermuth for sid2-2 genotyping protocol; Dr. Alexandra Jones for mass spectrometry analyses; Kelsey Mescher, Drs. Tanya Falbel, and Bationa Shahollari for technical assistance; Dr. Neil Hoffman for calnexin antibody; and Dr. Gary Weisman and laboratory for discussion.

REFERENCES

1. Boller, T., and Felix, G. (2009) *Annu. Rev. Plant Biol.* **60,** 379–406
2. Nicaise, V., Roux, M., and Zipfel, C. (2009) *Plant Physiol.* **150,** 1638–1647
3. Liew, F. Y., Xu, D., Brint, E. K., and O'Neill, L. A. J. (2005) *Nat. Rev. Immunol.* **5,** 446–458
4. Lorrain, S., Vailleau, F., Balagué, C., and Roby, D. (2003) *Trends Plant Sci.* **8,** 263–271
5. Falbel, T. G., Koch, L. M., Nadeau, J. A., Segui-Simarro, J. M., Sack, F. D., and Bednarek, S. Y. (2003) *Development* **130,** 4011–4024
6. Levivier, E., Goud, B., Souchet, M., Calmels, T. P., Mornon, J. P., and Callebaut, I. (2001) *Biochem. Biophys. Res. Commun.* **287,** 688–695
7. Allaire, P. D., Marat, A. L., Dall'Armi, C., Di Paolo, G., McPherson, P. S., and Ritter, B. (2010) *Mol. Cell* **37,** 370–382
8. Marat, A. L., and McPherson, P. S. (2010) *J. Biol. Chem.* **285,** 10627–10637
9. Del Villar, K., and Miller, C. A. (2004) *Proc. Natl. Acad. Sci. U.S.A.* **101,** 4210–4215
10. Niwa, S., Tanaka, Y., and Hirokawa, N. (2008) *Nat. Cell Biol.* **10,** 1269–1279
11. Sato, M., Sato, K., Liou, W., Pant, S., Harada, A., and Grant, B. D. (2008) *EMBO J.* **27,** 1183–1196
12. Lee, J. H., Terzaghi, W., Gusmaroli, G., Charron, J. B., Yoon, H. J., Chen, H., He, Y. J., Xiong, Y., and Deng, X. W. (2008) *Plant Cell* **20,** 152–167
13. Heese, A., Hann, D. R., Gimenez-Ibanez, S., Jones, A. M., He, K., Li, J., Schroeder, J. I., Peck, S. C., and Rathjen, J. P. (2007) *Proc. Natl. Acad. Sci. U.S.A.* **104,** 12217–12222
14. Wildermuth, M. C., Dewdney, J., Wu, G., and Ausubel, F. M. (2001) *Nature* **414,** 562–565
15. Yang, S., and Hua, J. (2004) *Plant Cell* **16,** 1060–1071
16. Rancour, D. M., Park, S., Knight, S. D., and Bednarek, S. Y. (2004) *J. Biol. Chem.* **279,** 54264–54274
17. Gómez-Gómez, L., Felix, G., and Boller, T. (1999) *Plant J.* **18,** 277–284
18. Ichimura, K., Casais, C., Peck, S. C., Shinozaki, K., and Shirasu, K. (2006) *J. Biol. Chem.* **281,** 36969–36976
19. Thordal-Christensen, H., Zhang, Z., Wei, Z., and Collinge, D. B. (1997) *Plant J.* **11,** 1187–1194
20. Fan, J., Crooks, C., and Lamb, C. (2008) *Plant J.* **53,** 393–399
21. Bartels, S., Anderson, J. C., González Besteiro, M. A., Carreri, A., Hirt, H., Buchala, A., Métraux, J. P., Peck, S. C., and Ulm, R. (2009) *Plant Cell* **21,** 2884–2897
22. Libault, M., Wan, J., Czechowski, T., Udvardi, M., and Stacey, G. (2007) *Mol. Plant-Microbe Interact.* **20,** 900–911
23. van Zanten, M., Snoek, L. B., Proveniers, M. C., and Peeters, A. J. (2009) *Trends Plant Sci.* **14,** 214–218
24. Chinchilla, D., Zipfel, C., Robatzek, S., Kemmerling, B., Nürnberger, T., Jones, J. D. G., Felix, G., and Boller, T. (2007) *Nature* **448,** 497–500
25. Zipfel, C., Kunze, G., Chinchilla, D., Caniard, A., Jones, J. D., Boller, T., and Felix, G. (2006) *Cell* **125,** 749–760
26. Zipfel, C., Robatzek, S., Navarro, L., Oakeley, E. J., Jones, J. D., Felix, G., and Boller, T. (2004) *Nature* **428,** 764–767
27. van Loon, L. C., Rep, M., and Pieterse, C. M. (2006) *Annu. Rev. Phytopathology* **44,** 135–162
28. Loake, G., and Grant, M. (2007) *Curr. Opin. Plant Biol.* **10,** 466–472
29. Nakagami, H., Soukupová, H., Schikora, A., Zársky, V., and Hirt, H. (2006) *J. Biol. Chem.* **281,** 38697–38704
30. Petersen, M., Brodersen, P., Naested, H., Andreasson, E., Lindhart, U., Johansen, B., Nielsen, H. B., Lacy, M., Austin, M. J., Parker, J. E., Sharma, S. B., Klessig, D. F., Martienssen, R., Mattsson, O., Jensen, A. B., and Mundy, J. (2000) *Cell* **103,** 1111–1120
31. Suarez-Rodriguez, M. C., Adams-Phillips, L., Liu, Y., Wang, H., Su, S. H., Jester, P. J., Zhang, S., Bent, A. F., and Krysan, P. J. (2007) *Plant Physiol.* **143,** 661–669
32. Jambunathan, N., Siani, J. M., and McNellis, T. W. (2001) *Plant Cell* **13,** 2225–2240
33. Melotto, M., Underwood, W., Koczan, J., Nomura, K., and He, S. Y. (2006) *Cell* **126,** 969–980
34. He, K., Gou, X., Yuan, T., Lin, H., Asami, T., Yoshida, S., Russell, S. D., and Li, J. (2007) *Curr. Biol.* **17,** 1109–1115
35. Su, S. H., Suarez-Rodriguez, M. C., and Krysan, P. (2007) *FEBS Lett.* **581,** 3171–3177
36. Lemaitre, B., Nicolas, E., Michaut, L., Reichhart, J. M., and Hoffmann, J. A. (1996) **86,** 973–983
37. Nühse, T. S., Bottrill, A. R., Jones, A. M., and Peck, S. C. (2007) *Plant J.* **51,** 931–940
38. Zhang, J., Shao, F., Li, Y., Cui, H., Chen, L., Li, H., Zou, Y., Long, C., Lan, L., Chai, J., Chen, S., Tang, X., and Zhou, J. M. (2007) *Cell Host Microbe* **1,** 175–185
39. Torres, M. A., Dangl, J. L., and Jones, J. D. G. (2002) *Proc. Natl. Acad. Sci. U.S.A.* **99,** 517–522
40. Lu, X., Tintor, N., Mentzel, T., Kombrink, E., Boller, T., Robatzek, S., Schulze-Lefert, P., and Saijo, Y. (2009) *Proc. Natl. Acad. Sci. U.S.A.* **106,** 22522–22527
41. Denoux, C., Galletti, R., Mammarella, N., Gopalan, S., Werck, D., De Lorenzo, G., Ferrari, S., Ausubel, F. M., and Dewdney, J. (2008) *Mol. Plant* **1,** 423–445
42. Tsuda, K., Sato, M., Glazebrook, J., Cohen, J. D., and Katagiri, F. (2008) *Plant J.* **53,** 763–775
43. Miyoshi, J., and Takai, Y. (2004) *Trends Mol. Med.* **10,** 476–480
44. Tanaka, M., Miyoshi, J., Ishizaki, H., Togawa, A., Ohnishi, K., Endo, K., Matsubara, K., Mizoguchi, A., Nagano, T., Sato, M., Sasaki, T., and Takai, Y. (2001) *Mol. Biol. Cell* **12,** 1421–1430
45. Mulherkar, N., Prasad, K. V., and Prabhakar, B. S. (2007) *J. Biol. Chem.* **282,** 11715–11721